Asian Journal of Chemistry; Vol. 25, No. 5 (2013), 2657-2662

ASIAN JOURNAL OF CHEMISTRY

http://dx.doi.org/10.14233/ajchem.2013.13603

Synthesis and Characteristic of Organic-Inorganic Hybrid Materials $Cu_2(OH)_{(4-x)}(C_{10}H_{17}O_2)_x \cdot zH_2O$

DESHAN ZHENG

School of Materials and Chemical Engineering, Xi'an Technological University, Xi'an 710032, P.R. China

Corresponding author: Fax: +86 29 83208197; Tel: +86 29 83208197; E-mail: deshan.zheng@sdu.edu.cn

(*Received*: 16 February 2012; *Accepted*: 19 November 2012) AJC-12423

In this paper, the ligand 3,7-dimethyl-6-octenoic acid was grafted in the inorganic groups layered hydroxy copper acetate through an anion exchange reaction. Combination of XRD, elemental analysis and TGA, the structure of these hybrid materials have been studied and characterized. The infrared, ultraviolet properties and magnetic spectra of these hybrid materials also discussed.

Key Words: Organic-inorganic hybrid materials, Layered compounds, Ion exchange reaction, Magnetic.

INTRODUCTION

Layered structure compounds, in particular, the anion exchangeable-layered structure compounds, is suitable for the design and preparation of new hybrid materials through the exchange of ions located in the interlayer space[1,2]. The new types of organic-inorganic hybrid materials obtained by such anionic exchange reactions not only retains the original features of the inorganic components, while introducing chirality *etc*., optical properties of organic molecules into the layered inorganic parts, that could be useful for chiral separation, recognition and photonic materials[3-6]. On the other hand, controlling the organization of the obtained materials nanoparticles can introduce additional functionality[7-9]. Therefore, these new types of organic-inorganic hybrid materials have been attracting more and more attention in recent years due to the reason that they can provide nice model systems for understanding the correlation between the structural and functional features[10,11].

The studies of Rikken and Raupach *et al*.[12-14] combined the chirality of organic ligands with the magnetic of inorganic components promote this research field developed rapidly. An important method they used is combination of magnetic properties of the inorganic components with the chirality of the organic ligands through strong chemical bonds (*i.e*., use the second class of hybrid materials combination of two phases by strong bonds such as covalent bond, *etc*.). Other similar examples reported in the literature are using of the transition metal oxalate complex with carboxylic acid or amino ligands *etc*., chiral functional groups, the formation of complexes or coordination compound is likely to be generation of optical materials with ferromagnetic compounds[15-19]. Due to this reason in this article the combination of inorganic layered transition metal hydroxy copper acetate with the organic chiral ligand 3,7-dimethyl-6-octenoic acid ($C_{10}H_{18}O_2$) as the main research.

In this paper, firstly the chiral ligand 3,7-dimethyl-6-octenoic acid was grafted in the inorganic groups layered hydroxy copper acetate through an anion exchange reaction, respectively, then the structure of these hybrid materials have been studied and characterized using XRD, elemental analysis and TGA. On this basis, the author discussed the spectral properties and magnetic properties of these obtained new types of organic-inorganic hybrid materials.

EXPERIMENTAL

Preparation of $Cu_2(OH)_3(CH_3COO)\cdot H_2O$: The copper hydroxide acetate $Cu_2(OH)_3(CH_3COO)\cdot H_2O$ is synthesized as described[20-22]. A blue-green powder was obtained by titration of 0.1 M solution of copper(II) acetate with 0.1 M solution of NaOH for a certain amount of molar ratio in an aqueous solution under argon at 60 ºC. After the reaction was completed, the precipitate was washed and dried at 50 ºC in air.

Preparation of $Cu_2(OH)_{(4-x)}(C_{10}H_{17}O_2)_x \cdot zH_2O$: In a typical synthesis procedure, a certain amount of 3,7-dimethyl-6-octenoic acid ($C_{10}H_{18}O_2$) was dissolved in an aqueous solution with vigorous stirring. The pH of the solution was kept *ca.* 9 by addition of NaOH aqueous solution slowly, then $Cu_2(OH)_3(CH_3COO)\cdot H_2O$ was added under argon at 60 ºC and the suspension was stirred at room temperature. After the reaction was completed, the solution was filter and the precipitate was washed several times with distilled water and absolute ethanol, respectively. The obtained powders were dried at 40 ºC in air.

The anion exchange reaction as follows:

$$Cu_2(OH)_3(CH_3CO_2)\cdot H_2O + 5\ eq\ L^- \xrightarrow[eq\cdot CH_3CO_2^-]{Ar} Cu_2(OH)_{(4-x)}(L)_x\cdot zH_2O + (5-x)\ eq\ L^- + x\ eq\cdot CH_3CO_2^-$$

Characterization: The samples were characterized by X-ray diffraction (XRD) using a Bragg-Brentano Siemens D 5000 diffractometer (CuK_α 1 = 1.540 598 Å). The morphologies of the as-synthesized powders were characterized by field emission scanning electron microscopy (FESEM JSM- 6700F). FT-IR studies were carried out with an ATI Mattson Genesis computer-driven instrument. UV/VIS/near-infrared studies were performed on a Perkin-Elmer Lambda 19 instrument. DTA/TGA experiments were performed on a Setaram TG 92 instrument (heating in air from 20-700 ºC at a rate of 5 ºC min^{-1}). Elemental analyses were performed *via* a Thermo-Finnigan EA 1112 setup (Service d'analyses, ICS, Strasbourg, France). The magnetic measurement of samples enclosed in a medical cap was performed with a superconducting quantum interference device (SQUID) magnetometer (Quantum Design model MPMS-XL).

Elemental analysis (%): calcd. for $Cu_2(OH)_{3.12}(RS\text{-}C_{10}H_{17}O_2)_{0.88}\cdot 1.83H_2O$ (m.w. = 362.50 g): C 29.29, H 5.55, Cu 36.06; found (%): C29.28, H 5.20, Cu 35.05. Calcd. (%) for $Cu_2(OH)_{3.12}(R\text{-}Cu_2(OH)_{3.19}(C_{10}H_{17}O_2)_{0.81}\cdot 1.85H_2O$ (m.w. = 351.47 g): C 27.61, H 5.38, Cu 36.19; found (%): C27.62, H 4.90, Cu 36.09. Calcd. (%) for $Cu_2(OH)_{3.12}(S\text{-}Cu_2(OH)_{3.19}(C_{10}H_{17}O_2)_{0.81}\cdot 1.85H_2O$ (m.w. = 352.35 g): C 27.74, H 5.40, Cu 36.07; found (%): C27.74, H 5.02, Cu 35.99.

RESULTS AND DISCUSSION

Powder X-ray structural analyses and scanning electron microscopy analyses: The XRD patterns of the as-prepared samples are shown in Fig. 1. Among the figure, the basal diffraction peak of anion-exchange samples $Cu_2(OH)_{(4-x)}(RS\text{-}C_{10}H_{17}O_2)_x\cdot zH_2O$ (plotted with Cu-RS), $Cu_2(OH)_{(4-x)}(S\text{-}C_{10}H_{17}O_2)_x\cdot zH_2O$ (plotted with Cu-S) and $Cu_2(OH)_{(4-x)}(R\text{-}C_{10}H_{17}O_2)_x\cdot zH_2O$ (plotted with Cu-R) move to the direction of the small angle comparison with the starting materials $Cu_2(OH)_3(CH_3CO_2)\cdot H_2O$ (diagram using Cu). The each d-values of diffraction peak were Cu (d_{001} = 0.936 nm, d_{002} = 0.468 nm, d_{003} = 0.312 nm), Cu-RS (d_{001} = 2.202 nm, d_{002} = 1.125 nm, d_{003} = 0.752 nm), Cu-S (d_{001} = 2.202 nm, d_{002} = 1.109 nm, d_{003} = 0.743 nm), Cu-R (d_{001} = 2.201 nm, d_{002} = 1.112 nm, d_{003} = 0.745 nm).

Fig. 1 shows that all the copper samples obtained by anion exchange reaction exhibit a lamellar structure as evidenced from their X-ray diffraction (XRD) patterns that show, in the low 2θ range, a series of well-oriented harmonic basal reflections that can be assigned to (00l) (l = 1, 2, 3). This corresponds to the stacking periodicity of the hydroxide-base layers (basal spacing). The average dimension of the interplanar crystal spacing and the grain size D001 of the 001 direction can be calculated according to the Scherrer formula as shown in Table-1, the results show that the average number of stacked layers along the (001) direction of the grain is *ca.* 11.

In addition, it also can be seen from the XRD patterns of all the copper compounds that the reflections at range 30-45° are both broad and show a similar asymmetry, which can be assigned to hk0 (in-plane) reflections. This phenomenon means

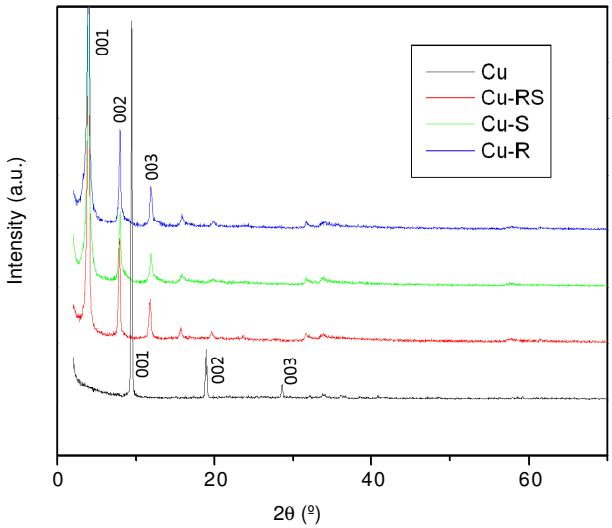

Fig. 1. XRD Spectra of copper hydroxide acetate: $Cu_2(OH)_3(CH_3COO)\cdot H_2O$ and the samples grafting of chiral 3,7-dimethyl-6-octenoic acid: $Cu_2(OH)_{(4-x)}(C_{10}H_{17}O_2)_x\cdot zH_2O$

TABLE-1
AVERAGE DIMENSION OF THE INTERPLANAR CRYSTAL SPACING, GRAIN SIZE AND THE AVERAGE NUMBER OF STACKED LAYERS ALONG THE (001) DIRECTION OF THE COPPER HYDROXIDE ACETATE: $Cu_2(OH)_3(CH_3COO)\cdot H_2O$ and THE SAMPLES GRAFTING OF CHIRAL 3,7-DIMETHYL-6-OCTENOIC ACID: $Cu_2(OH)_{(4-x)}(C_{10}H_{17}O_2)_x\cdot zH_2O$

Samples	d001 (nm)	Grain size (nm)	Average number of stacked layers along the (001) direction
Cu-RS	2.202	24.922	11
Cu-S	2.202	22.373	10
Cu-R	2.201	24.083	11

that the structure within the layers does not vary too much. Actually, such variation is essentially because of the necessary adaptation of the molecular area of each metal ion to the molecular area of the grafted anions[23,24]. This feature has been observed for α-nickel hydroxide and α-cobalt hydroxide and so on relatively layered hydroxides due to the turbostratic behaviour, *i.e.*, the layers stacking ordered in two dimensions, but their layers are orientationally disordered[25-28]. From the SEM images of samples aggregation shape shown in Fig. 2, can also observe this phenomenon, which shows that the as-prepared all these hybrid materials appear as fold thin platelet shaped but irregular arrangement microcrystals in agreement with their lamellar and orientationally disordered character of their structure.

UV-visible reflectance structural studies and infrared spectroscopic properties: The organic-inorganic layered hybrid materials has both electron donor (ligand) and the electron acceptor (metal ions), for such compounds, electronic absorption spectra can generally be divided into two parts of the central ion bands (*d-d*, *f-f*) at the low energy side (long wavelength) and the charge transfer bands mainly at the high-energy side (short wavelength).

Present copper hydroxide-based hybrid compounds are consistent with such metallic environments[29] and show the two characteristic bands (Fig. 3). The most intense absorption is observed in the range of 260-270 nm and corresponds undoubtedly to charge transfer (O → Cu).The second absorption

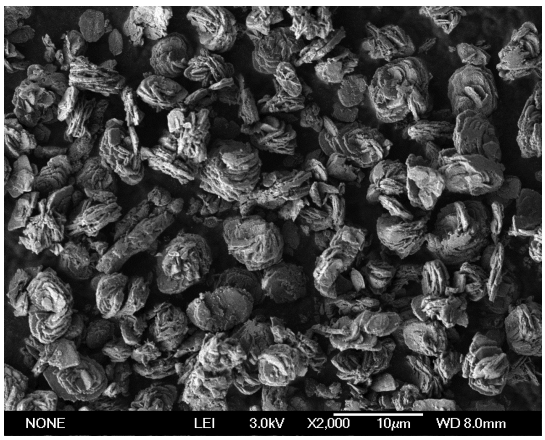

(a)

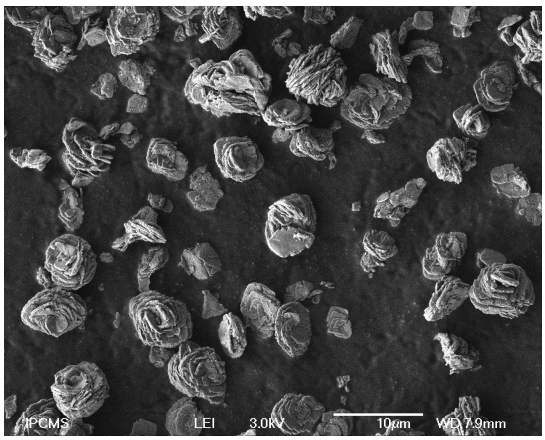

(b)

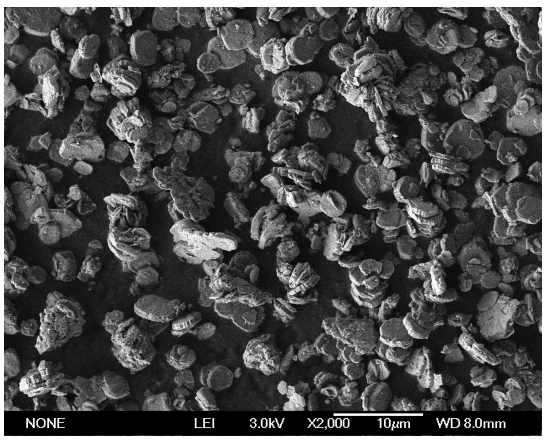

(c)

Fig. 2. SEM images of the as-prepared samples (a) $Cu_2(OH)_{(4-x)}(RS\text{-}C_{10}H_{17}O_2)_x{\cdot}zH_2O$ (b) $Cu_2(OH)_{(4-x)}(S\text{-}C_{10}H_{17}O_2)_x{\cdot}zH_2O$ (c) $Cu_2(OH)_{(4-x)}(R\text{-}C_{10}H_{17}O_2)_x{\cdot}zH_2O$

band appears between 690 and 740 nm mainly is attributed to $^2E_g \rightarrow {}^2T_{2g}$ among the d^9 transition bands (*d-d*) of the central ion Cu(II).

The structure of the exchanged layered hybrid compounds was also investigated by Fourier transform infrared (FT-IR) spectroscopy (Fig. 4). The large and broad absorption band in the range of 3700-3000 cm^{-1} is the signature of the stretches of hydroxyl groups of water molecules and hydrogen-bonded hydroxyl groups. Further, additional bands occur in the range

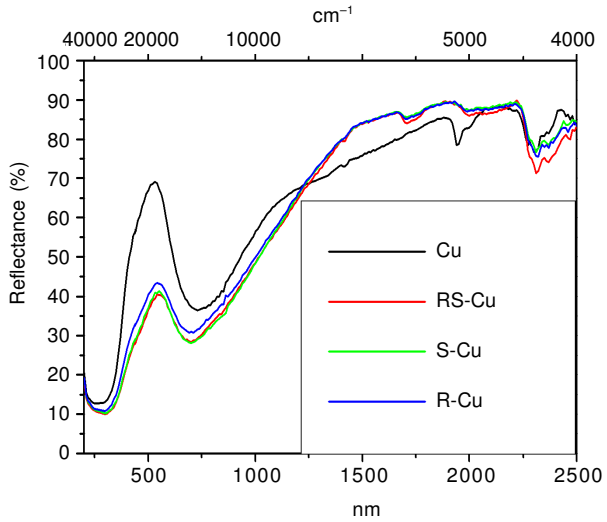

Fig. 3. UV-VIS reflectance spectra of compounds the copper hydroxide acetate: $Cu_2(OH)_3(CH_3COO){\cdot}H_2O$ and the samples grafting of chiral 3,7-dimethyl-6-octenoic acid: $Cu_2(OH)_{(4-x)}(C_{10}H_{17}O_2)_x{\cdot}zH_2O$

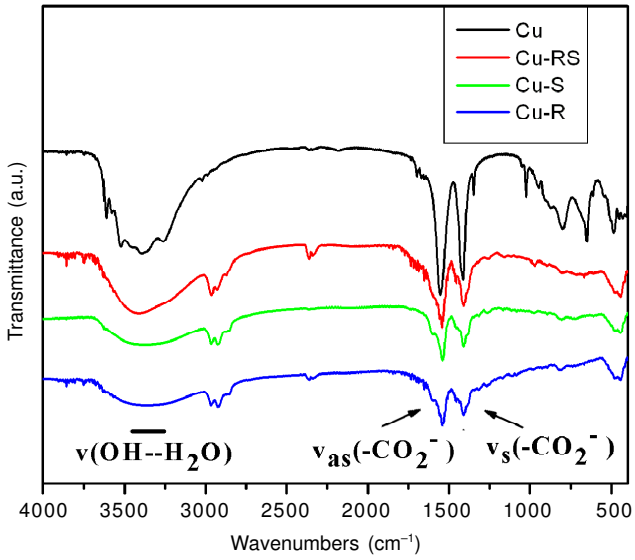

Fig. 4. IR spectra of the copper hydroxide acetate: $Cu_2(OH)_3(CH_3COO){\cdot}H_2O$ and the samples grafting of chiral 3,7-dimethyl-6-octenoic acid: $Cu_2(OH)_{(4-x)}(C_{10}H_{17}O_2)_x{\cdot}zH_2O$

of 3000-2800 cm^{-1} may be due to the symmetric and asymmetric stretching vibration of the saturation CH_3 and CH_2. Finally, a quite strong feature appears in the range 1575-1525 cm^{-1} can be assigned to the antisymmetric stretching $\nu_{as}COO$ and in the range 1420-1370 cm^{-1} attributed to ν_sCOO of of CO_2- in carboxylate doublet group, respectively (Table-2). For the starting compound $Cu_2(OH)_3(CH_3COO){\cdot}H_2O$, the two bands and the difference between its as $\Delta\nu = \nu_{as}\text{-}\nu_s$ = 1551-1412 cm^{-1} = 139 cm^{-1}. In the case of the exchanged compounds, after deprotonation and coordination to a metal ion, this doublet is still present and slightly shifted about to 1539 and 1408 cm^{-1}. While the difference between the two bands also slightly shifted from 131 to 135 cm^{-1}, suggests a bridging carboxylate[30] (*i.e.*, one of the two oxygen atoms of the carboxylate groups linked with a copper(II) ion, the other in a strong hydrogen bond with a neighboring hydroxy ion due to charge balance between the organic and inorganic sub-networks).

TABLE-2
ANTISYMMETRIC STRETCHING (ν_{as}COO), SYMMETRIC STRETCHING (ν_sCOO) VIBRATIONS AND THE FREQUENCY DIFFERENCE ($\Delta\nu$) OF CO^{2-} IN METAL HYDROXIDE ACETATE, THE CARBOXYL FUNCTIONAL GROUPS IN THE THE SAMPLES

Samples	ν_{as}COO (cm^{-1})	ν_sCOO (cm^{-1})	$\nu = \nu_{as} - \nu_s$ (cm^{-1})
$Cu(Cu_2(OH)_3(CH_3CO_2)\cdot H_2O)$	1551	1412	139
Cu-RS	1541	1406	135
Cu-S	1539	1408	131
Cu-R	1539	1408	131

Thermogravimetric and differential thermal analysis: Figs. 5 and 6 show the thermogravimetric and differential thermal (TG and DTA) curves of all the copper hydroxide-based compounds in a temperature range from 25-700 ºC conducted in air with the final decomposition product being CuO.

The results of TG/DTA for racemic hybrid compound $Cu_2(OH)_{(4-x)}(RS\text{-}C_{10}H_{17}O_2)_x\cdot zH_2O$ are presented in Fig. 5 and exhibit three step decomposition. The first step gives a broad endothermic curve in the DTA from 25-155 ºC, which including two endothermic peaks located at 77 and 132 ºC correspond to dehydration of water molecules from the interlayers and $Cu_2(OH)_{(4-x)}(C_{10}H_{17}O_2)_x$ dissociated into $Cu_2O_x(OH)_{(4-2x)}$ and $(C_{10}H_{18}O_2)_x$, respectively. The corresponding mass loss in thermogravimetric curve (TG) is characterized by a certain

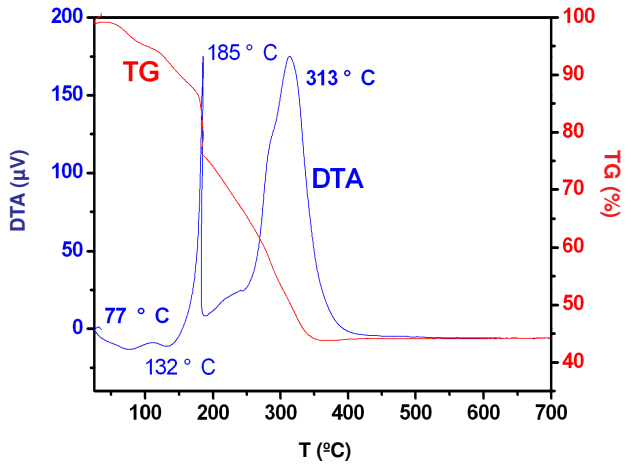

Fig. 5. TG/DTA data of $Cu_2(OH)_{(4-x)}(RS\text{-}C_{10}H_{17}O_2)_x\cdot zH_2O$

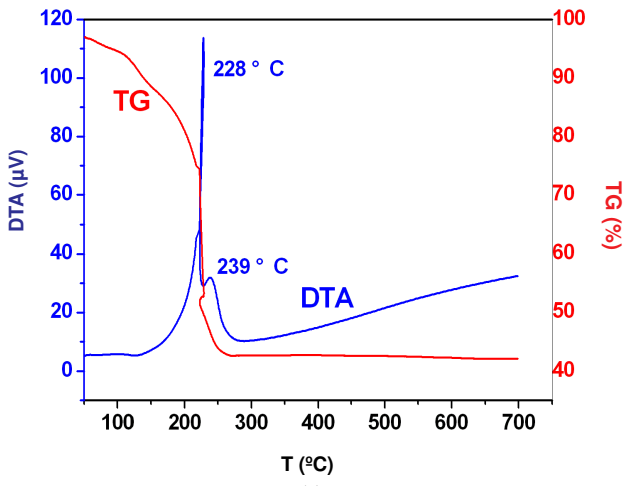

(a)

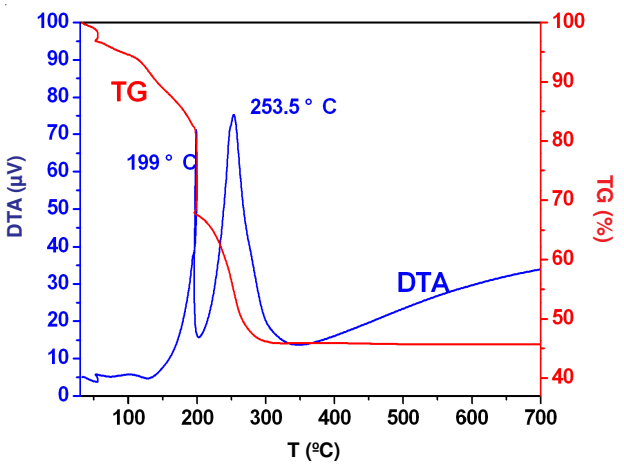

(b)

Fig. 6. TG/DTA data of $Cu_2(OH)_{(4-x)}(S(a)/R(b)\text{-}C_{10}H_{17}O_2)_x\cdot zH_2O$

slope of the weight loss process of 9.48 %, which is consistent with the theoretical water content mass loss of 9.09 % of the stoichiometric formula $Cu_2(OH)_{3\cdot12}(C_{10}H_{17}O_2)_{0.88}\cdot1.83H_2O$. It can be best represented by the two following reactions:

$$Cu_2(OH)_{(4-x)}(C_{10}H_{17}O_2)_x\cdot zH_2O \rightarrow Cu_2(OH)_{(4-x)}(C_{10}H_{17}O_2)_x + zH_2O \quad (1)$$

(Endothermic, up to *ca.* 77 ºC).

$$Cu_2(OH)_{(4-x)}(C_{10}H_{17}O_2)_x \rightarrow Cu_2O_x(OH)_{(4-2x)} + (C_{10}H_{18}O_2)_x \quad (2)$$

(Endothermic, up to *ca.* 132 ºC).

The next step gives a sharp exothermic curve in the DTA from 155-189 ºC, accompanied by a rapid weight loss of 13.84 % (calcd. 14.63 %) in the thermogravimetric curve (TG). The thermal decomposition product is CuO identified by powder XRD. The following reaction is expected.

$$Cu_2O_x(OH)_{(4-2x)} \rightarrow 2CuO + (2-x)H_2O \quad (3)$$

(Exothermic, up to *ca.* 185 ºC).

In the final step, a distinct exothermic peak can be observed on the differential thermal analysis (DTA) curve about 313 ºC associated with a gradual mass loss process of 31.73 % (calcd. 41.01 %) according to the TG curve in a temperature range of 189-393 ºC. It should be assigned to the decomposition of intercalated $(C_{10}H_{18}O_2)_x$ ligands[31]. The strong exothermic phenomenon is attributed to the combustion of the ligands $(C_{10}H_{18}O_2)_x$ to formation of CO_2 and H_2O. The corresponding reaction should be:

$$(C_{10}H_{18}O_2)_x + 27xO_2 \rightarrow 10xCO_2 + 9xH_2O \quad (4)$$

(Exothermic, up to *ca.* 313 ºC).

Based on above the TG/DTA data analysis of the $Cu_2(OH)_{(4-x)}(RS\text{-}C_{10}H_{17}O_2)_x\cdot zH_2O$, it is suggested that for TG/DTA curves of $Cu_2(OH)_{(4-x)}(S\text{-}C_{10}H_{17}O_2)_x\cdot zH_2O$ and $Cu_2(OH)_{(4-x)}(R\text{-}C_{10}H_{17}O_2)_x\cdot zH_2O$, they have a similar weight loss and endothermic/exothermic curve (Fig. 6). But in the last step, due to accompanied by a strongly combustion of ligands exothermic, making the exothermic peak changes, located at 239 and 253 ºC for, respectively.

Magnetic properties: Temperature variation of the magnetic susceptibility, χ was measured using a SQUID magnetometer between 300 and 1.8 K under a magnetic field

of H = 5000 Oe. The $\chi T = f(T)$ curves for the Cu-based hybrid compounds are presented in Fig. 7.

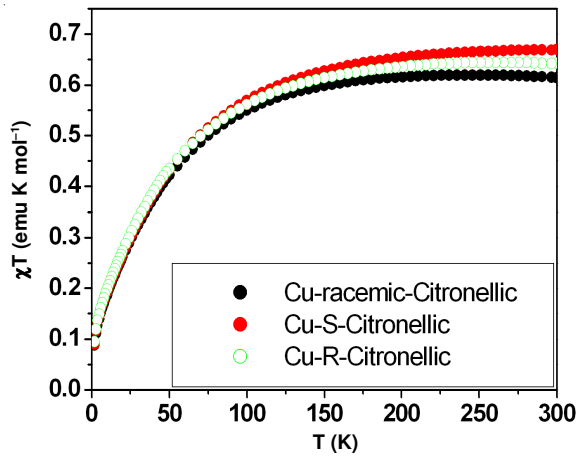

Fig. 7. Magnetic behaviour as χT *vs*. T plots of compounds $Cu_2(OH)_{4-x}(C_{10}H_{17}O_2)_x \cdot zH_2O$

It can be seen from the figure that the curves for the Cu-based hybrid compounds are similar exhibiting a two-dimensional antiferromagnetic behaviour over the whole temperature range, as illustrated by the continuous decay of the χT product from 0.64 emu K mol^{-1} at 300 K to 0.09 emu K mol^{-1} at 1.8 K. There is no evidence of bulk ordering in the investigated temperature range. This behaviour is consistent with the low-temperature magnetization *versus* field measurements (Fig. 8). It can be seen that the magnetization curves are characteristic of an antiferromagnetism, whether they are in low fields or high fields, generally exhibiting an approximated linear and very small slow increase without hysteresis. The magnetization value at 5 T is very low, only 0.15 μ_B and far from the saturation value.

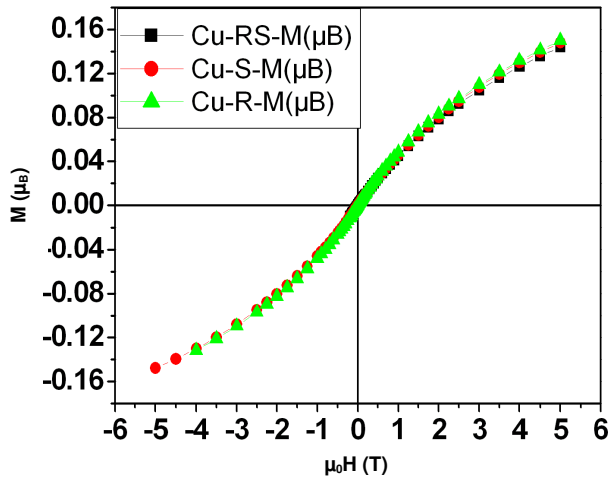

Fig. 8. Field dependent magnetization of compounds $Cu_2(OH)_{4-x}(C_{10}H_{17}O_2)_x \cdot zH_2O$

The above studies of the magnetic behaviour of these hybrid materials show a slightly change compared with that of the starting material $Cu_2(OH)_3(CH_3CO_2) \cdot H_2O$,which is an antiferromagnetic, with weakly ferromagnetic Cu(II) planes and antiferromagnetic interplane coupling, promoting a metamagnetic system reported by Suzuki *et al*.[32] performed in the same ambient pressure conditions. The different magnetic features are related to a structural modification of the inorganic magnetic layers. Indeed, the hydroxide-based layer are known to be very sensitive to any structural modification, which can induce significant changes in the distances and angle along the Cu-O-Cu bridges and consequently in the exchange pathways, giving a change of sign (antiferromagnetic or ferromagnetic) of the interaction[33]. In this paper, for $Cu_2(OH)_{4-x}(C_{10}H_{17}O_2)_x \cdot zH_2O$ series, the increases linearly with the aliphatic chain length and different large separation between magnetic layers just are responsible for the above observed magnetic behaviours compared with that of the starting material $Cu_2(OH)_3(CH_3CO_2) \cdot H_2O$.

Conclusion

We have successfully prepared the copper-based organic-inorganic hybrid compounds by exchange reaction, using the $Cu_2(OH)_3(CH_3CO_2) \cdot H_2O$ as starting material. It is shown that the exchangeable anion $CH_3CO_2^-$ may be substituted by large organic species (3,7-dimethyl-6-octenoic acid anion) at room temperature, through a mechanism of swelling of the inorganic network. Then the structure and magnetic properties of obtained hybrid compounds have been characterized. XRD and SEM studies reveal that the hybrid compounds displays a layered topology, the crystal grain size *ca.* 24 nm, the average number of stacked layers along the (001) direction of the grain is *ca.* 11. From a magnetic point of view, it has been shown that this family of layered hybrid compounds exhibiting an antiferromagnetic behaviour differ from that of the copper hydroxyl acetate at same conditions due to the grafted ligands were increases linearly with the aliphatic chain length and bring about different large separation between magnetic layers.

ACKNOWLEDGEMENTS

This work is supported by the President Fund of Xi'an Technological University, China (No. XAGDXJJ1009).

REFERENCES

1. B.C. Wu, C.C. Zhang and W.G. Zhang, Organic-Inorganic Hybrid Materials and Applications, Chemical Industry Press, Beijing, pp. 5-286 (2005).
2. M.C. Hong, *Chin. J. Inorg. Chem*., **1**, 24 (2002).
3. A. Gabashvili, D.D. Medina, A. Gedanken and Y. Mastai, *J. Phys. Chem. B*, **111**, 11105 (2007).
4. B.F.G. Johnson, S.A. Raynor, D.S. Shephard, T. Mashmeyer, J.M. Thomas, G. Sankar, S. Bromley, R. Oldroyd, L. Gladden and M. D.. Mantle, *Chem. Commun*., 1167 (1999).
5. S. Fireman-Shoresh, I. Popov, D. Avnir and S. Marx, *J. Am. Chem. Soc*., **127**, 2650 (2005).
6. I. Hodgkinson and Q.H. Wu, *Adv. Mater*., **13**, 889 (2001).
7. Z.H. Nie, A. Petukhova and E. Kumacheva, *Nat. Nanotechnol*., **5**, 15 (2010).
8. N.A. Kotov and F. Stellacci, *Adv. Mater*., **20**, 4221 (2008).
9. C.L. Chen and N.L. Rosi, *Angew. Chem. Int. Ed*., **49**, 1924 (2010).
10. A. Rujiwatra, C.J. Kepert, J.B. Claridge, M.J. Rosseinsky, H. Kumagai and M. Kurmoo, *J. Am. Chem. Soc*., **123**, 10584 (2001).
11. H. Shimizu, M. Okubo, A. Nakamoto, M. Enomoto, N. Kojima, *Inorg. Chem*., **45**, 10240 (2006).
12. G.L.J.A. Rikken and E. Raupach, *Nature*, **390**, 493 (1997).
13. G.L.J.A. Rikken and E. Raupach, *Nature*, **405**, 932 (2000).
14. L.D. Barron, *Nature*, **405**, 895 (2000).
15. N.S. Ovanesyan, V.D. Makhaev, S.M. Aldoshin, P. Gredin, K. Boubekeur, C. Train and M. Gruselle, *Dalton Trans*., **18**, 3101 (2005).

16. A. Beghidja, G. Rogez, P. Rabu, R. Welter and M. Drillon, *J. Mater. Chem*., **16**, 2715 (2006).
17. X. Meng, C. Qin, X. L. Wang, Z.M. Su, B. Li and Q.H. Yang, *Dalton Trans*., **40**, 9964 (2011).
18. M. Minguet, D. Luneau, E. Lhotel, V. Villar, C. Paulsen, D.B. Amabilino and J. Veciana, *Angew. Chem. Int. Ed*., **41**, 586 (2002).
19. K. Inoue, H. Imai, P.S. Ghalsasi, K. Kikuchi, M. Ohba, H. O-kawa and J.V. Yakhmi, *Angew. Chem. Int. Ed*., **40**, 4242 (2001).
20. V. Laget, M. Drillon, C. Hornick, P. Rabu, F. Romero, P. Turek, R. Ziessel, *J. Alloys Comp*., **262-263**, 423 (1997).
21. V. Laget, C. Hornick, P. Rabu and M. Drillon, *J. Mater. Chem*., **9**, 169 (1999).
22. V. Laget, C. Hornick, P. Rabu, M. Drillon and R. Ziessel, *Coord. Chem. Rev*., **178-180**, 1533 (1998).
23. C. Hornick, P. Rabu and M. Drillon, *Polyhedron*, **19**, 259 (2000).
24. J.M. Rueff, J.F. Nierengarten, P. Gilliot, A. Demessence, O. Cregut, M. Drillon and P. Rabu, *Chem. Mater*., **16**, 2933 (2004).
25. M. Dixit, G.N. Subbanna and P.V. Kamath, *J. Mater. Chem*., **6**, 1429 (1996).
26. F. Cavani and F. Trifiro, *Catal. Today*, **11**, 173 (1991).
27. R.S. Jayashree and P.V. Kamath, *J. Mater. Chem*., **9**, 961 (1999).
28. Y. Zhu, H. Li, Y. Koltypin and A. Gedanken, *J. Mater. Chem*., **12**, 729 (2002).
29. A.B.P. Lever, Inorganic Electronic Spectroscopy, Elsevier, Amsterdam, edn. 2 (1984).
30. K. Nakamoto, Infrared and Raman Spectra of Inorganic and Coordination Compounds, John Wiley & Sons, New York, edn. 4, pp. 124-232 (1986).
31. H.C. Zeng, Z.P. Xu and M. Qian, *Chem. Mater*., **10**, 2277 (1998).
32. K. Suzuki, J. Haines, P. Rabu, K. Inoue and M. Drillon, *J. Phys. Chem. C*, **112**, 19147 (2008).
33. O. Kahn, Molecular Magnetism, VCH Publishers, Weinheim (1993).